CELL TECHNOLOGIES IN BIOLOGY AND MEDICINE

Modeling and Immunohistochemical Analysis of C6 Glioma *In Vivo*

V. P. Chekhonin, V. P. Baklaushev, G. M. Yusubalieva, K. A. Pavlov, O. V. Ukhova, and O. I. Gurina

Translated from *Kletochnye Tehnologii v Biologii i Medicine*, No. 2, pp. 65-73, April, 2007
Original article submitted February 1, 2006

A reproducible *in vivo* model of C6 glioma was developed in Wistar rats. Analysis of histological preparations showed similar morphology of rat C6 glioma and human glioblastoma. The formation of a glial border at the periphery of the glioma, consisting of GFAP-positive reactive astrocytes, was shown by the immunohistochemical method. The border appeared on day 8 after implantation, astrogliosis was observed until animal death (day 28). Reactive astrocytes with branched processes surrounded not only the primary glioma focus, but also all sites of tumor invasion in the nervous tissue. Expression of EBA (blood-brain barrier marker) was disturbed and synthesis of AMVB1 (endothelial antigen) increased in neoplastic endotheliocytes, which suggested pronounced functional restructuring of the blood-tumor barrier in comparison with the blood-brain barrier. The phenomenon of predominant expression of GFAP and AMVB1 in the tumor tissue can be used for the development of systems for targeted drug transport into the tumor by means of appropriate antibodies.

Key Words: *C6 glioma; immunohistochemistry of the brain; glia fibrillar acid protein; endothelial barrier antigen*

The prognosis of multiform glioblastoma and medulloblastoma (the most invasive poorly differentiated brain tumors) is extremely unfavorable because of their rapid progress and inefficiency of traditional surgical, radio-, and chemotherapeutic methods [21]. The mean survival of patients with these diseases from the moment of diagnosis is about one year [17].

C6 glioma induced in rats serves as a model of human glioblastoma in experimental studies [4]. Rapidly progressing cell strain of this glioma was obtained in Wistar—Furth rats by induction of carcinogenesis with N,N'-nitrosomethylurea [12]. C6 glioma is very close to human multiform glioblastoma by morphology, characteristics of invasive growth, and spectrum of expressed proteins [1,20]. The spectrum of proteins expressed by C6 glioma includes basal membrane and cell adhesion proteins, tissue proteolytic enzymes responsible for degradation of intercellular matrix during invasion, signal proteins, growth factors and their receptors maintaining high level of tumor cell proliferation and stimulating angiogenesis [4].

Changes in the protein spectrum specific of poorly differentiated brain tumors are observed in tumor capillary endotheliocytes and in the glial cells surrounding the tumor. For example, intensive neoangiogenesis is associated with increased synthesis

Laboratory of Immunochemistry, V. P. Serbsky National Research Centre for Social and Forensic Psychiatry, Federal Agency for Health Care and Social Development, Moscow

of receptors for tyrosine kinase (TKRs), growth factors (VEGF, FGF, PDGF, angiopoietin-1 and -2), and integrins ($\alpha_3\beta_1$, $\alpha_5\beta_1$) [14]. During this process some normally absent pathological proteins appear in the endothelium: PV-1 (plasmalemmal vesicle associated protein-1) [2], PAL-E (pathologische anatomie leiden-endothelium) [8,13], MECA 32 [5], and Cx43 connexin [3]. The changes involving the glial cells are characterized, among other things, by intense proliferation of fibrillar astrocytes directly participating in modulation of the blood-tumor barrier permeability [10]. However, the phenomenon of reactive astrogliosis caused by primary brain tumor is poorly understood [4].

The aim of our study was the development of a reproducible model of C6 glioma in rats and dynamic immunohistochemical analysis of GFAP (glial fibrillary acidic protein) and endothelial antigens EBA and AMVB1 during the development of glioma. Endothelial barrier antigen (EBA), recognized by SMI-71 monoclonal antibodies (Sternberger Inc.), is a specific marker of the cerebral capillary barrier endothelium [7,15]. The expression of EBA is in high correlation with functional integrity of the blood-brain barrier (BBB) and is disordered in diseases associated with BBB impairment [9,11, 16,22].

Monoclonal antibodies 2mB6 visualizing endothelial protein AMVB1 were obtained at Laboratory of Immunochemistry of V. P. Serbsky Center by immunization with preparations of brain capillary membrane fraction. This antigen is also present in the cerebral endothelium, but is not directly associated with BBB functions, because it was also detected in non-barrier endotheliocytes in other organs.

The choice of GFAP, EBA, and AMVB1 proteins is explained by the need to characterize reactive astrogliosis accompanying the tumor and to evaluate molecular changes in neoplastic endotheliocytes, which could be used for the development of systems for targeted transport of drugs into glioma capillary system.

MATERIALS AND METHODS

Preparation of C6 glioma in culture. An aliquot of C6 glioma cells (10^6) frozen in liquid nitrogen was rapidly defrosted, washed from dimethylsulfoxide by centrifugation, resuspended in 12 ml complete medium (DMEM, 20% fetal serum, 2 mM L-glutamine, 25 mM HEPES, 10,000 U/ml antibiotic-antimycotic), and inoculated in culture flasks (Costar). After attaining confluence (Fig. 1), glioma cells were harvested by enzymatic dissociation (TryPLE Express; Invitrogen) for 10 min at 37°C, washed from fetal serum in Hanks solution, resuspended in dissociating buffer (Invitrogen), and counted in a Goryaev chamber. Cell viability was evaluated by trypan blue staining. Aliquots (0.5×10^6 cells in 1 ml DMEM with antibiotics) were prepared and stored for 3-4 h at 4°C until stereotaxic injection into the brain. For reliable location of tumor cell invasion in brain sections, some aliquots were labeled with fluorescent tracer CFDA SE (carboxyfluorescein diacetate succinylimidyl ether; excitation and emission peaks at 492 and 515 nm, respectively) using a Vybrant CFDA SE Cell Tracer Kit (Invitrogen) according to manufacturer's instruction.

Glioblastoma was modeled *in vivo* by stereotaxic intracerebral implantation of C6 cells. The study was carried out in 30 adult female Wistar rats weighing 200-220 g at the beginning of the experiment. Glioma cells (5×10^5 per rat) were implanted under ketamine narcosis to the caudoputamen area using a Narishige stereotaxic device according to Swanson's Brain Atlas coordinates [18]: AP -1; L 3.0; V 4.5; TBS -2.4 mm. The cells were injected with a Hamilton microsyringe connected to an infusomat at a rate of 3 μl/min (10-15 μl).

Histological studies were carried out 2 h, 3, 8, 15, 21, and 28 days after implantation. The rats were deeply narcotized and perfused with 4% paraformaldehyde through the aorta; serial sections (40 μ) were made on a freezing microtome (Reichart). The preparations for general morphological analysis were stained by several methods: after Nissl (0.1% cresyl violet in 0.1 M acetate buffer, pH 3.3) and with toluidine blue in the same buffer. Combined staining with toluidine blue and 0.1% vanadium acid fuchsin (VAF) after I. V. Victorov [19] was used for visualization of necrotic foci in the tumor.

Immunohistochemical analysis of C6 glioma preparations was carried out using SMI-71 (Sternberger Monoclonal Inc.), 2mB6 and anti-GFAP monoclonal antibodies (Laboratory of Immunochemistry, V. P. Serbsky National Research Centre for Social and Forensic Psychiatry). For immunoperoxidase visualization, anti-species biotinilated antibodies BA2000 (Vector Lab.) were used as the second antibodies with subsequent visualization of the antigen—antibody reaction with avidin—biotin—peroxidase complex (ABC elite, Vector Lab.). Diaminobenzidine (0.01%) served as the chromogenic substrate for peroxidase. For immunofluorescent analysis, brain sections treated with primary antibodies were incubated with anti-murine IgG labeled with Texas Red (Sigma, excitation and emission peaks of 589 and 615 nm, respectively). Cell nuclei were post-stained with DAPI (Invitrogen; excitation and emission peaks of 358 and 461 nm,

respectively). The sections were examined under fluorescent microscope (Leica MS) and TCS SP2 scanning laser confocal microscope (Leica MS) at N. N. Koltsov Institute of Developmental Biology, Russian Academy of Sciences.

RESULTS

Histological analysis revealed tumors in all animals. The tumor size corresponded to the period elapsed after injection of glioma cells (Fig. 2). Two hours after injection the size of glioma focus together with the injection track was 1.9±0.2% of the total area of the caudoputamen section; by day 21 the size of glioma increased more than 30-fold (61.8± 9.76% of total section area). In 3 rats surviving until day 28, glioma occupied 84.9±2.9% area of hemisphere sections, metastasized, and destroyed the basal nuclei, corpus callosum, and lower layers of the cerebral cortex. Pronounced intracranial dislocation and compensatory shrinkage of the contralateral hemisphere were observed (Fig. 2, *d*). The shape and size of glioma cells varied; cell nuclei were polymorphic (Fig. 3, *b*), which corresponded to histological picture of human multiform glioblastoma.

Due to high content of ribonucleoproteins, glioma cells are highly chromophilic and are more in-

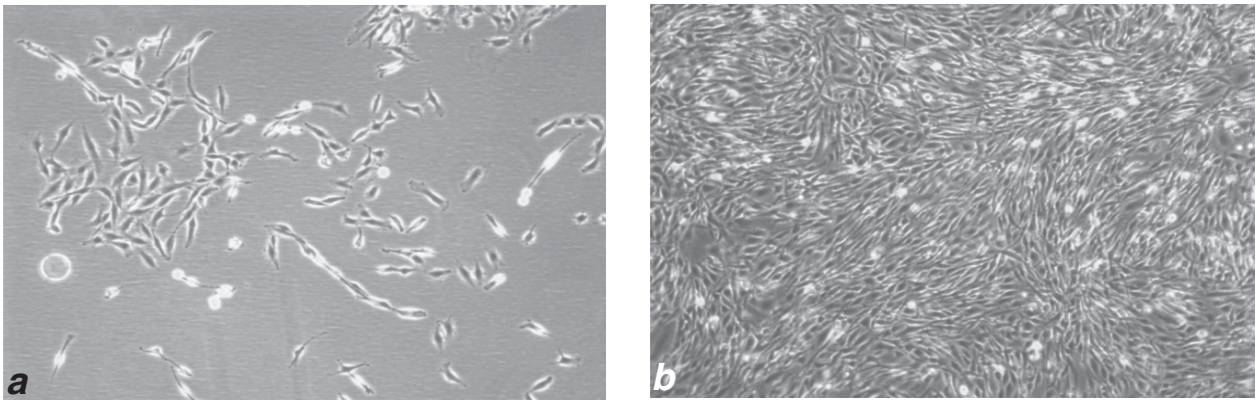

Fig. 1. Culture of C6 glioma (phase contrast; ×200). *a*) 24 h after defrosting; *b*) C6 cell monolayer after 3-5-day culturing.

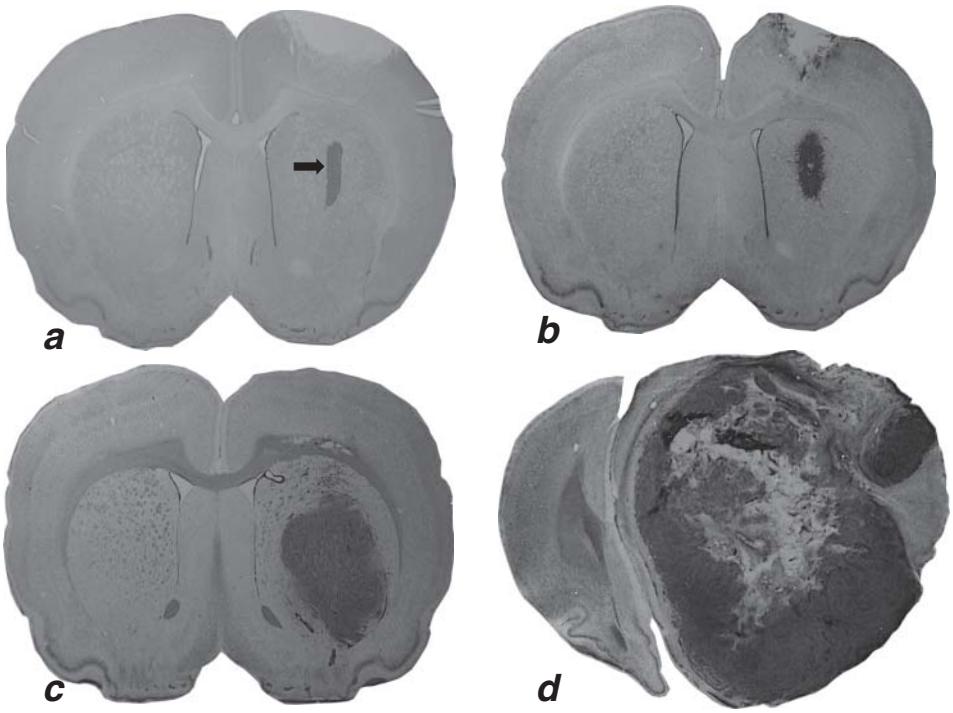

Fig. 2. Implanted C6 glioma in rat caudoputamen 2 h (*a*), 3 (*b*), 15 (*c*), and 28 (*d*) days after implantation (×20). Staining with 0.1% toluidine blue and VAF. Arrow shows the site of implantation (*a*).

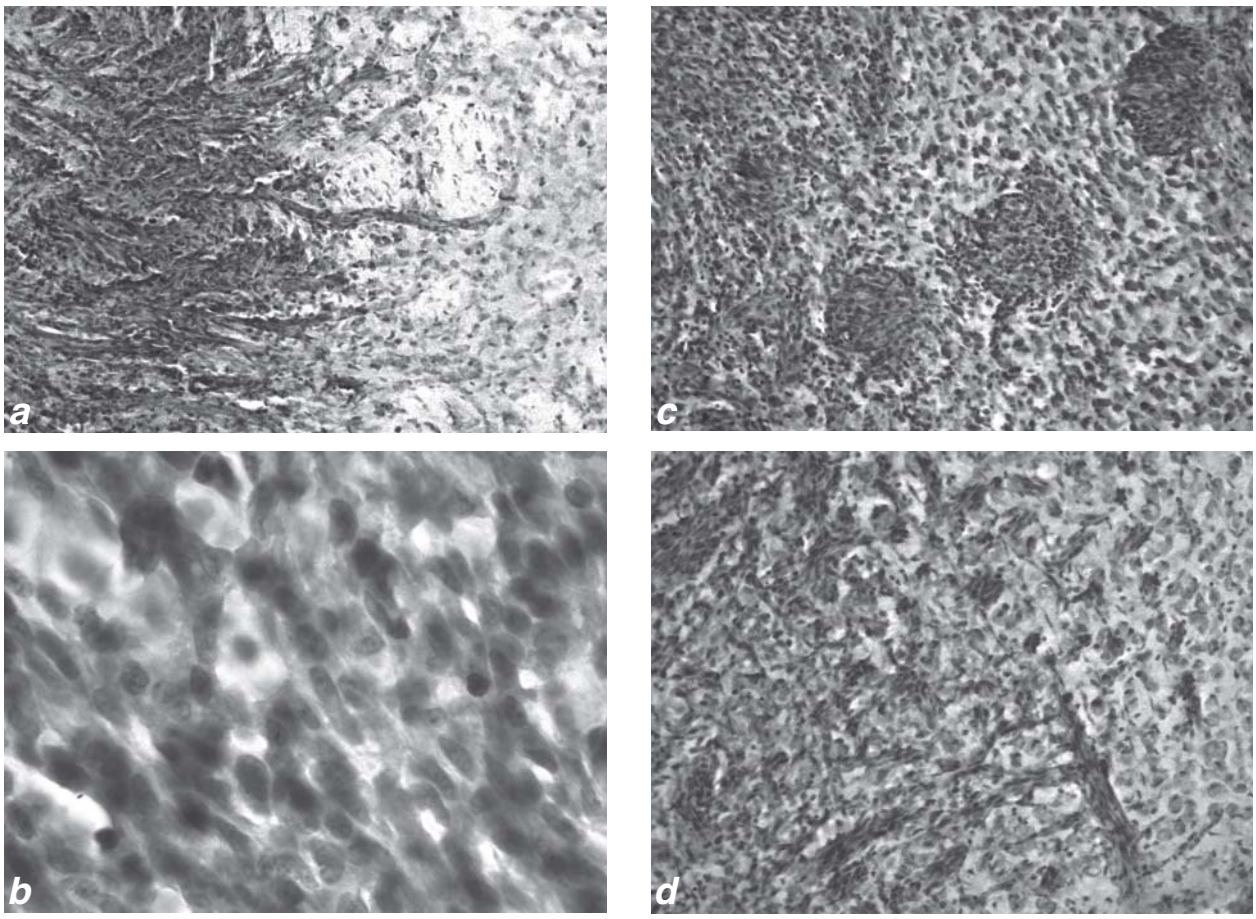

Fig. 3. Histogram of C6 glioma on brain preparations stained with cresyl violet and toluidine blue. *a*) general view (×100); *b*) polymorphism of glioma cell nuclei, oil immersion (×1000); *c*) perivasal invasion (arrows); *d*) perineural invasion (arrow).

tensively stained with cresyl violet and toluidine blue compared to normal nervous tissue. Hence, clearly differentiated main tumor focus and large foci of invasion were seen under a light microscope (Fig. 3, *c*). The tumor spread along the perivasal and perineural space (Fig. 3, *a*, *d*).

Staining with VAF visualized dead acidophilic cells selectively stained garnet. Combined staining with VAF and toluidine blue detected zones of central necrosis sometimes transforming into cysts (Fig. 2, *d*; Fig. 4, *a*) and numerous smaller foci containing degenerating tumor cells (Fig. 4, *b*).

Preliminary labeling of glioma cells with CFDA SE vital tracer showed that active invasion of tumor cells into intact nervous tissue started as early as on day 3 after implantation and peaked after 1 week.

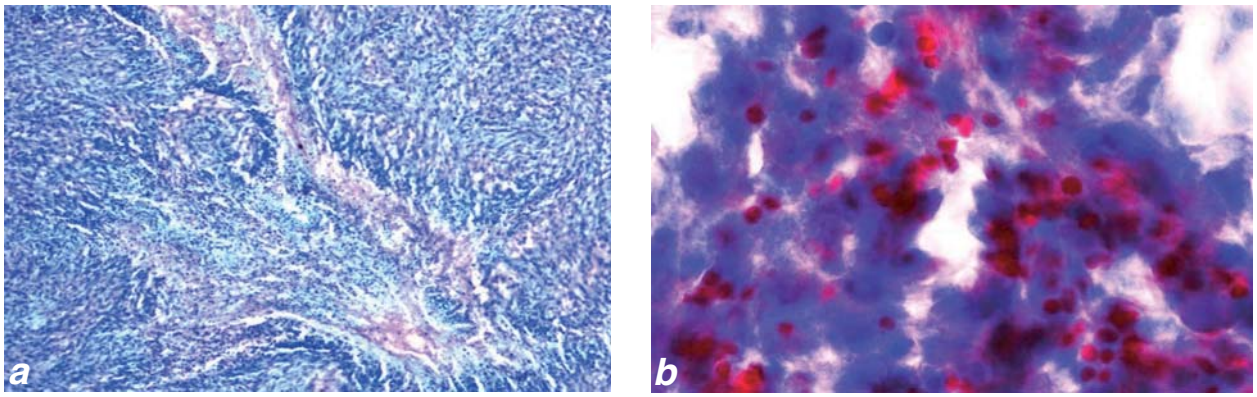

Fig. 4. Necrosis of glioma cells on day 21 after implantation. *a*) central necrosis zone (×100); *b*) small foci of necrosis (VAF staining; oil immersion, ×1000).

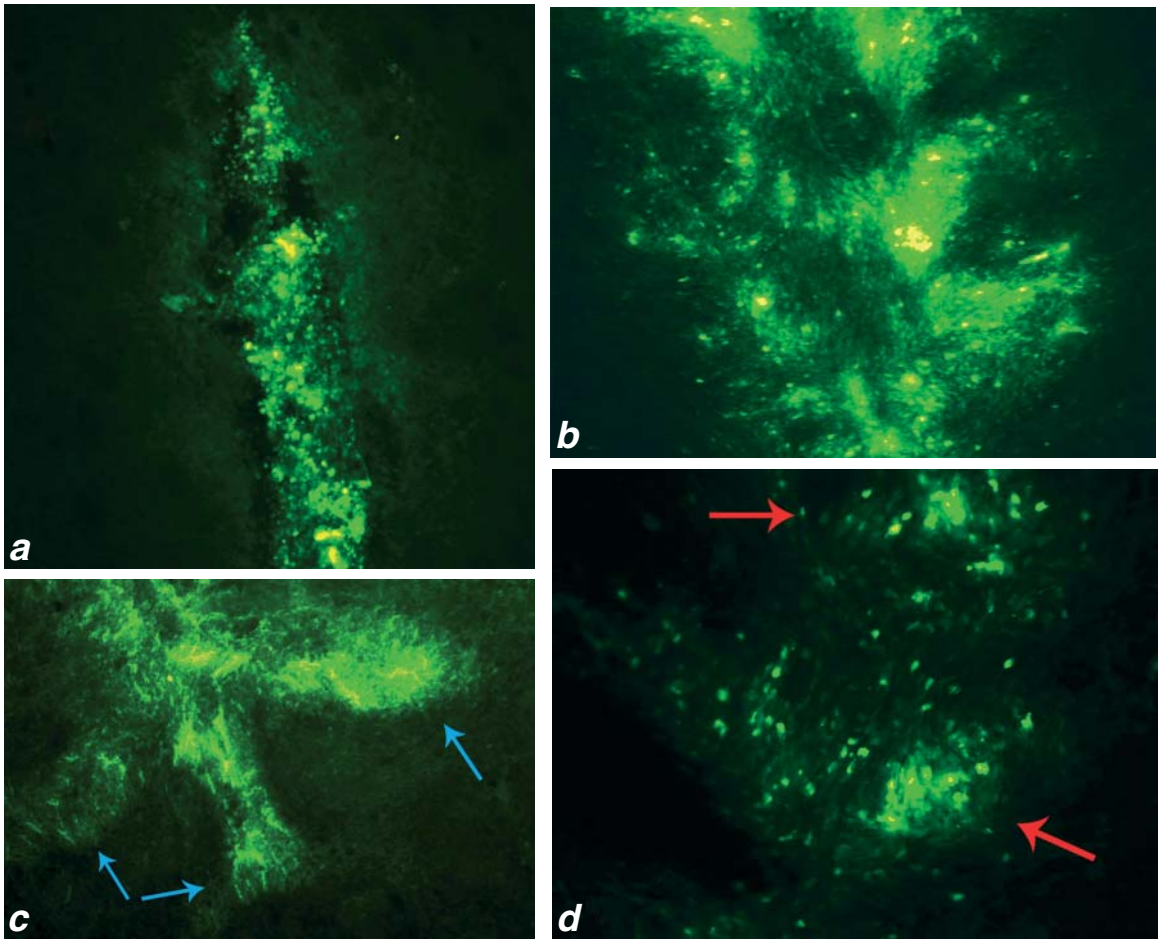

Fig. 5. Fluorescence of implanted glioma cells labeled with CFDA SE tracer. *a*) day 3 after injection (×100); *b*) day 8 after injection (×200); *c*) perivasal infiltration on day 8 (arrows, ×200); *d*) distant foci of invasion (arrows, ×400).

On day 8 after implantation, glioma cells with the tracer were detected at a distance of 500 μ from the implantation site (Fig. 5). CFDA SE fluorescence was observed up to day 28, but its intensity decreased as a result of division of labeled cells.

Immunohistochemical analysis demonstrated significant differences in the expression of GFAP, EBA, and AMVB1 in tumor and normal nervous tissue. Antibodies to GFAP visualized glial border around the glioma, which contained many GFAP-positive reactive astrocytes with branched processes forming a network (Fig. 6). The formation of the border was recorded on day 8 after implantation of glioma cells and then throughout the entire experiment until day 28, when glioma destroyed the corpus callosum and grew into the cerebral cortex, after which reactive astrocytes were detected in all cortical layers (Fig. 6, *d*).

As the tumor grew, some astrocytes were surrounded by glioma cells and their processes oriented parallel to the direction of glioma growth. These astrocytes were visualized in the thickness of the tumor in glioma preparations up to day 15 (Fig. 6, *a*). It seems that these cells died with further growth of glioma, because no GFAP-positive structures were detected deeper than 150-200 μ from tumor edge at later terms. All invasion foci, forming at different distances from the site of implantation, were surrounded by reactive fibrillar astrocytes with branched processes (Fig. 7). Glioma cells were never stained with antibodies to GFAP during any period of development, this being in line with the common theory according to which poorly-differentiated tumor cells cannot express tissue-specific proteins of intermediate filaments [4].

The expression of endothelial antigens in rapidly growing tumor capillaries also changed significantly. There was virtually no EBA detected by SMI-71 antibodies during the early periods after implantation (Fig. 8, *c*, *d*). In normal tissue around the tumor, the cell still produced EBA, but the intensity of this synthesis decreased in sites closer to the tumor focus. The absence of EBA in endotheliocytes of neoplastic capillaries indicated im-

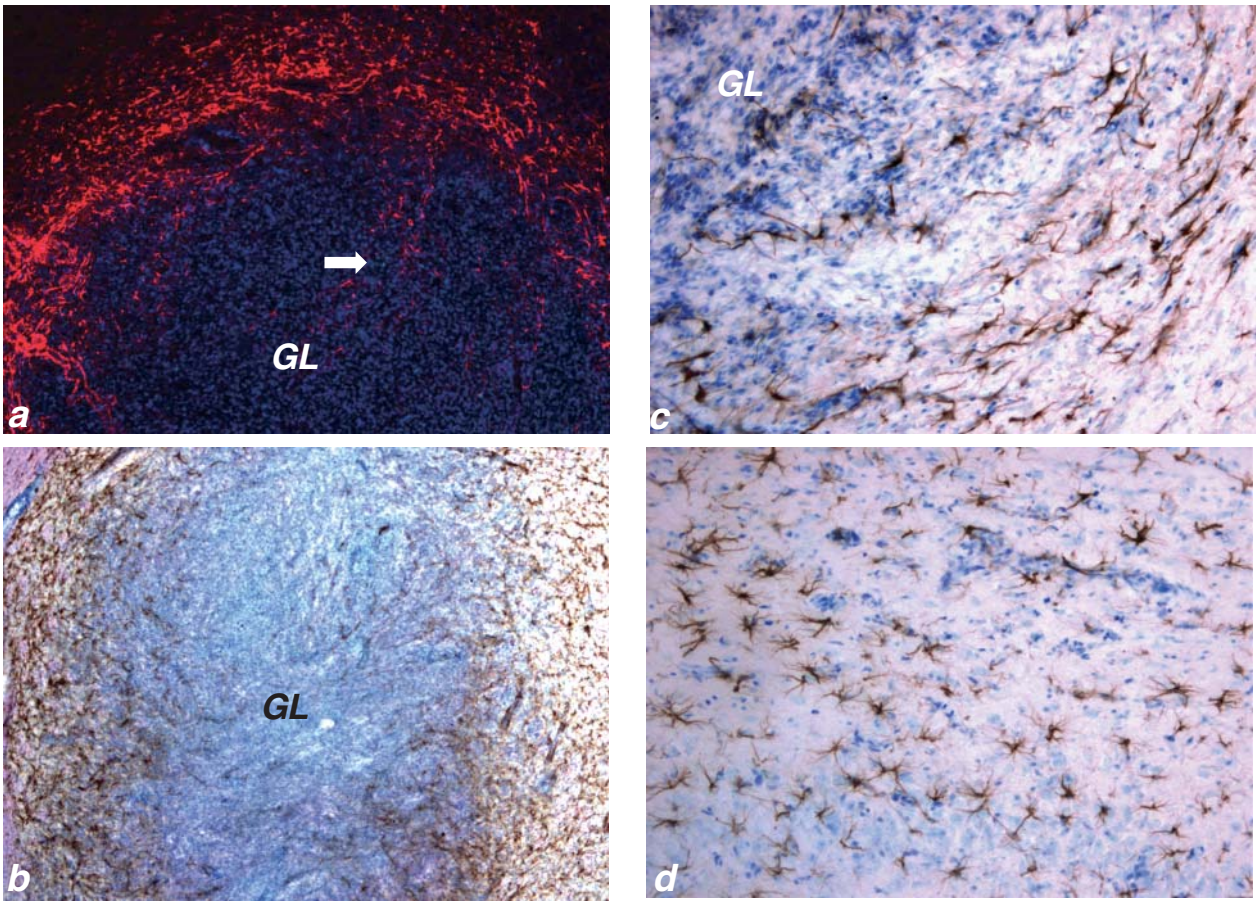

Fig. 6. Immunofluorescent (*a*) and immunoperoxidase (*b-d*) visualization of GFAP-positive reactive astrocytes around the glioma. *a*) second antibodies (arrow shows astrocytes penetrating into the tumor; Texas Red staining, nuclei were post-stained with DAPI, ×100); *b-d*) biotinilated second antibodies and ABC complex (nuclei were post-stained with 0.1% toluidine blue, ×50 (*b*); ×200 (*c*, *d*). GL: glioma.

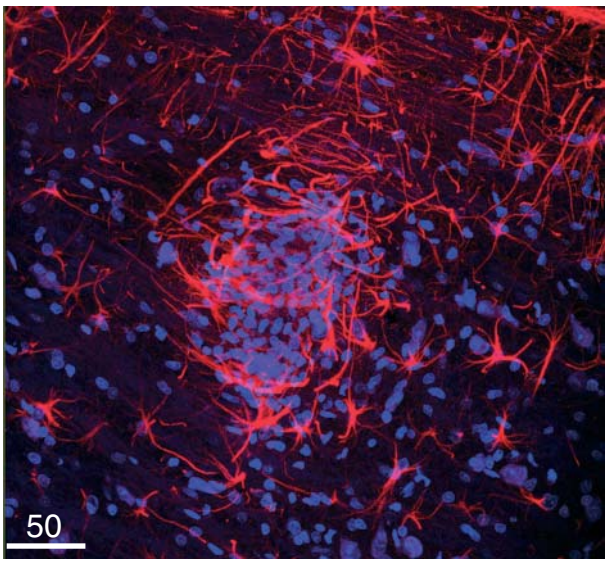

Fig. 7. Laser scanning confocal microscopy of reactive GFAP-positive astrocytes surrounding the foci of C6 glioma invasion. Second antibodies stained with Texas Red, cell nuclei were post-stained with DAPI (maximum projection, 1280×1024).

paired expression of proteins involved in the formation and maintenance of BBB functions.

In addition to the absence of EBA, intensive expression of AMVB1 endothelial antigen recognized by MAb 2mB6 was detected starting from day 8 after implantation (Fig. 8, *a*, *b*). These antibodies visualized branched vascular network of the tumor, whereas the caudoputamen area in normal cerebral parenchyma contained only solitary positive capillaries. Later (on days 21 and 28), when foci of central necrosis appeared in the tumor, the intensity of staining with MAb 2mB6 somewhat decreased both in tumor tissue and retained intact parenchyma; however, similarly as GFAP-positive astroglial border, AMVB1-positive capillaries were present in the tumor throughout the entire experiment.

According to the data of confocal microscopy, AMVB1 antigen is presumably located on the abluminal and/or basal membrane of endotheliocytes (Fig. 9). Immunohistochemical analysis showed maximum expression of this protein in the cerebellar cortex and brain stem (Fig. 10), while in the

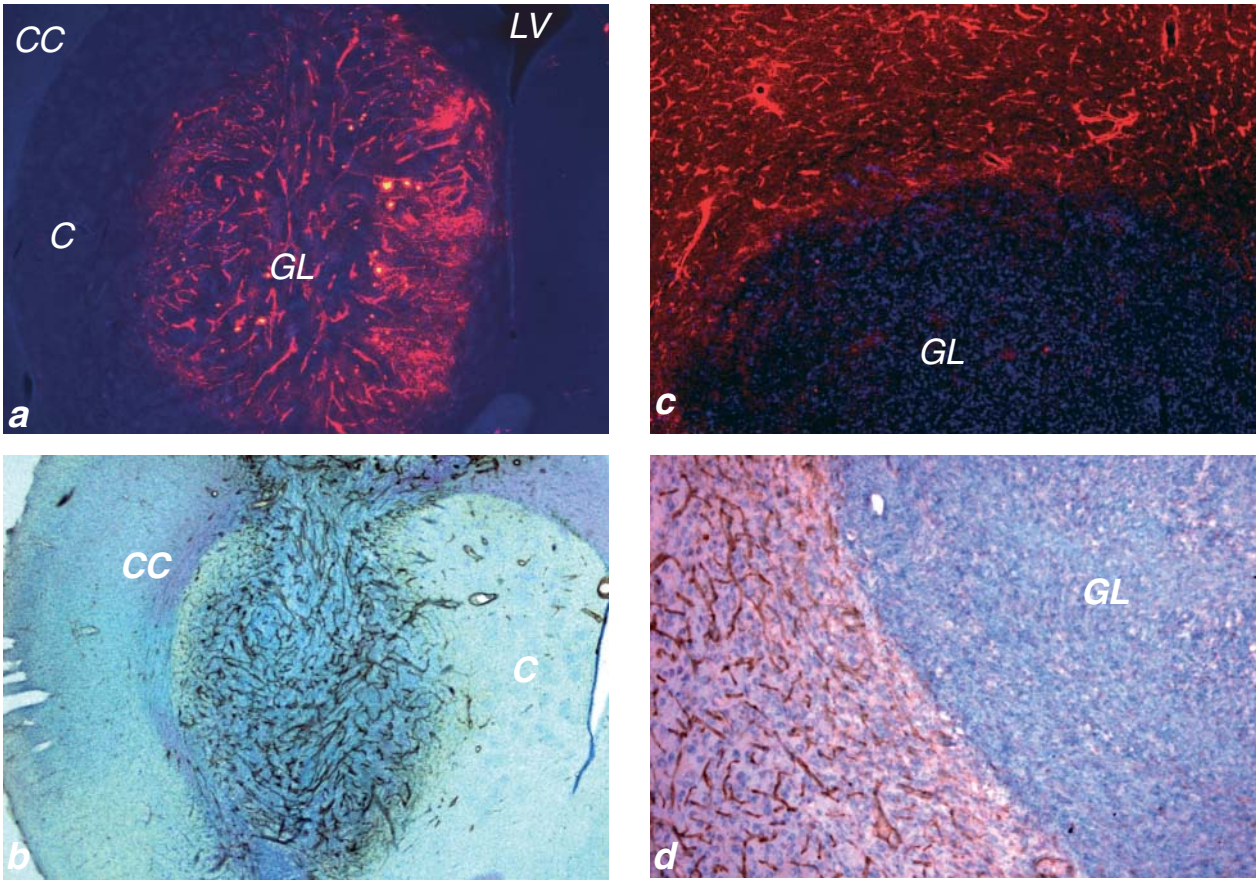

Fig. 8. Immunofluorescent analysis of endothelial markers in experimental C6 glioma. *a*, *b*: immunofluorescent (*a*) and immunoperoxidase (*b*) visualization of AMVB1 with MAb 2mB6; *c*, *d*: immunofluorescent (*c*) and immunoperoxidase (*d*) visualization of EBA endothelial barrier antigen with MAb SMI-71. *a*, *c*) Texas Red staining of second antibodies, cell nuclei post-stained with DAPI; *b*, *d*) biotinilated second antibodies and avidin—biotin—peroxidase complex. GL: glioma; CC: corpus callosum; LV: lateral ventricle; C: caudoputamen.

neocortex this protein was normally almost absent. Increased synthesis of AMVB1 can indicate functional restructuring of the basal membrane and endothelium in neoplastic capillaries.

Hence, a reproducible model of rat C6 glioma, maximally approximating human glioblastoma by histological characteristics was obtained and characterized. The main morphological features of C6 glioma are pronounced heterogeneity of cells, rapid invasive growth with perivasal and perineural infiltration, and formation of necrotic foci and cysts at late stages.

Dynamic analysis of reactive astrogliosis around glioma demonstrated the phenomenon of formation of a border from reactive GFAP-positive astrocytes starting from day 8 of glioma development until animal death. The most valuable fact is detection of reactive astrocytes around all invasion foci at the tumor periphery. This suggests a more precise detection of the glioma borderline by means of labeled antibodies to GFAP, on the one hand, and the development of a system of target transport of diagnostic and therapeutic preparations into the tumor on the base of antibodies to GFAP, on the other.

The expression of EBA and AMVB1 endothelial antigens during the development of experimental C6 glioma is characterized. Pronounced disorders in the synthesis of endothelial markers of BBB was detected, which presumably serves as the molecular basis of abnormal permeability of the blood-tumor barrier. In addition, the expression of AMVB1 (endotheliocyte abluminal membrane protein) increases significantly during neoplastic angiogenesis in comparison with normal cerebral capillaries. This phenomenon can also be used for the development of systems for target transport of diagnostic agents and drugs to the glioma focus.

The authors are grateful to Dr. A. S. Kholanskii (Institute of Human Morphology, Russian Academy of Medical Sciences) for kind gift of the preparation, to K. P. Ionova (V. P. Serbsky Institute of Forensic Medicine) for assistance in handling laboratory animals, to Prof. I. V. Victorov and Dr. I. P. Lazarenko (V. P. Serbsky Institute of Forensic Medicine) for consultations on histological analysis, and to Dr. E. B. Tsitrin (N. N. Koltsov Institute of

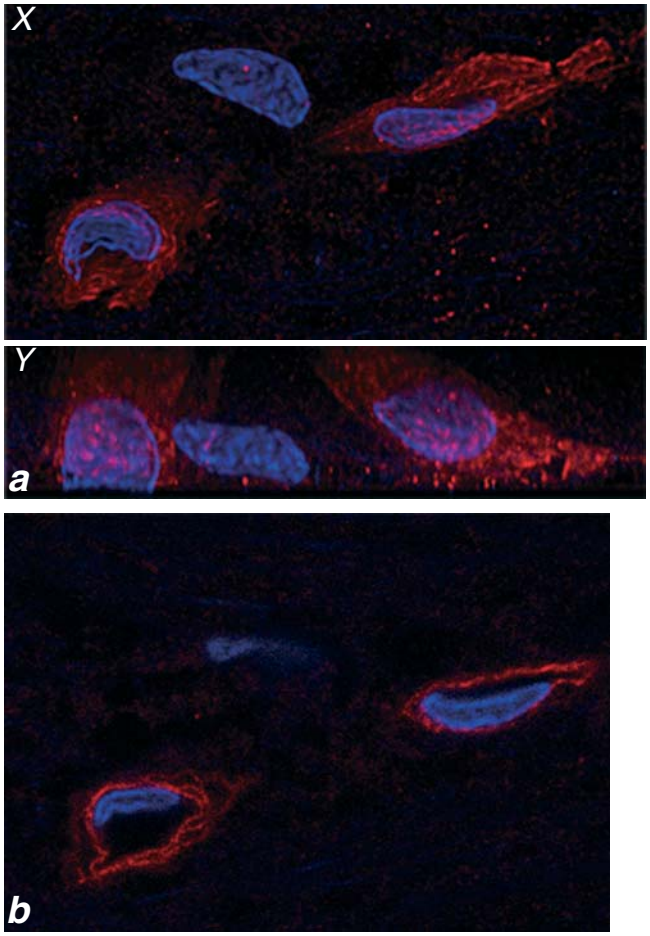

Fig. 9. Scanning laser confocal microscopy: subcellular location of AMVB1 endothelial antigen. *a*) maximum projection by *X*, *Y*, *Z* axes; *b*) brain capillary cross-section. Texas Red staining of second antibodies, cell nuclei post-stained with DAPI.

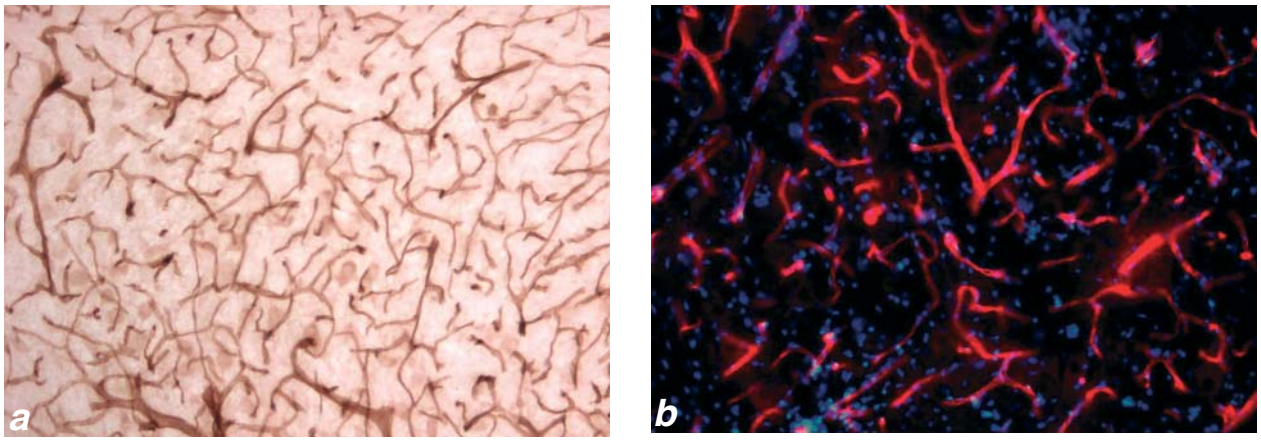

Fig. 10. Immunohistochemical analysis of AMVB1 endothelial antigen recognized by 2mB6 MAb in rat cerebelum (×100). *a*) second biotinilated antibodies (visualization with avidin—biotin—peroxidase complex); *b*) second antibodies stained with Texas Red, cell nuclei were post-stained with DAPI.

Developmental Biology, Russian Academy of Sciences) for assistance in confocal microscopy.

REFERENCES

1. R. N. Auer, R. F. Del Maestro, and R. Anderson, *Can. J. Neurol. Sci.*, **8**, No. 4, 325-331 (1981).
2. E. B. Carson-Walter, J. Hampton, E. Shue, *et al.*, *Clin. Cancer Res.*, **11**, No. 21, 7643-7650 (2005).
3. M. Errede, V. Benagiano, F. Girolamo, *et al.*, *Histochem. J.*, **34**, Nos. 6-7, 265-271 (2002).
4. B. Grobben, P. P. De Deyn, and H. Slegers, *Cell Tissue Res.*, **310**, No. 3, 257-270 (2002).
5. R. Hallmann, D. N. Mayer, E. L. Berg, *et al.*, *Dev. Dyn.*, **202**, No. 4, 325-332 (1995).

6. B. T. Hawkins and R. D. Egleton, *J. Neurosci. Methods*, **151**, No. 2, 262-267 (2006).
7. J. G. Lawrenson, M. N. Ghabriel, A. R. Reid, *et al.*, *J. Anat.*, **186**, Pt. 1, 217-221 (1995).
8. S. Leenstra, D. Troost, P. K. Das, *et al.*, *Cancer*, **72**, No. 10, 3061-3067 (1993).
9. B. Lin and M. D. Ginsberg, *Brain Res.*, **865**, No. 2, 237-244 (2000).
10. N. Nagano, H. Sasaki, M. Aoyagi, and K. Hirakawa, *Acta Neuropathol.* (Berlin), **86**, No. 2, 117-125 (1993).
11. M. Perdiki, M. Farooque, A. Holtz, *et al.*, *Ibid.*, **96**, 8-12 (1998).
12. J. H. Sampson, G. E. Archer, and D. D. Bigner, *Neurosurgery: The Scientific Basis of Clinical Practice*, Eds. A. Clockard *et al.*, Oxford (1999).
13. R. O. Schlingemann, P. Hofman, G. F. Vrensen, and H. G. Blaauwgeers, *Diabetologia*, **42**, No. 5, 596-602 (1999).
14. J. C. Soria, J. Fayette, and J. P. Armand, *Ann. Oncol.*, **15**, Suppl. 4, iv223-iv227 (2004).
15. N. H. Sternberger and L. A. Sternberger, *Proc. Natl. Acad. Sci. USA*, **84**, No. 22, 8169-8173 (1987).
16. N. H. Sternberger, L. A. Sternberger, M. W. Kies, and C. R. Shear, *J. Neuroimmunol.*, **21**, Nos. 2-3, 241-248 (1989).
17. L. A. Stewart, *Lancet*, **359**, 1011-1018 (2002).
18. L. W. Swanson, *Brain Maps: Structure of the Rat Brain*, 2nd ed., Amsterdam (1998).
19. I. V. Victorov, K. Prass, and U. Dirnagl, *Brain Res. Brain Res. Protoc.*, **5**, No. 2, 135-139 (2000).
20. I. R. Whittle, D. C. Macarthur, G. P. Malcolm, *et al.*, *J. Neuro-oncol.*, **36**, No. 3, 231-242 (1998).
21. M. R. Zalutsky, *J. Nucl. Med.*, **46**, Suppl. 1, 151S-156S (2005).
22. C. Zhu, M. N. Ghabriel, P. C. Blumbergs, *et al.*, *Exp. Neurol.*, **169**, No. 1, 72-82 (2001).